

## Filling of carbon nanotubes for bio-applications

S. Costa<sup>1</sup>, E. Borowiak-Palen<sup>\*1</sup>, A. Bachmatiuk<sup>1</sup>, M. H. Rummeli<sup>1,2</sup>, T. Gemming<sup>2</sup>,  
and R. J. Kaleńczuk<sup>1</sup>

<sup>1</sup> Centre of Knowledge Based Nanomaterials and Technologies, Institute of Chemical and Environment Engineering, Szczecin University of Technology, Poland

<sup>2</sup> Leibniz Institute for Solid State and Materials Research, Dresden, Germany

Received 24 April 2007, revised 2 August 2007, accepted 21 September 2007

Published online 8 November 2007

PACS 61.46.Fg, 68.37.Lp, 79.20.Uv, 81.07.De, 81.15.Fg

Carbon nanotubes (CNT) provide a smart carrier system on the nanometer scale. The system can be used as a template for ferromagnetic fillers. Such a molecular hybrid is a promising potential candidate for the controlled heating of tumour tissue at the cellular level. This is a key reason why it is important to optimize the synthesis route of metal filled carbon nanotubes with regards bulk scale synthesis and purity. In the current study we present multiwalled carbon nanotubes filled with  $\alpha$ -iron phase (Fe-MWCNT). The influence of acid treatment on the stability of the filling and the sample purity is also presented. High resolution transmission microscopy, its Energy dispersive X-Ray spectroscopy (EDX) and electron energy-loss spectroscopy (EELS) modes have been applied for the analysis of the morphology and chemical composition of the samples. The phase of iron nanowires encapsulated into the carbon nanotubes was determined with selected area electron diffraction (SAED) on a local scale.

© 2007 WILEY-VCH Verlag GmbH & Co. KGaA, Weinheim

### 1 Introduction

One of the most interesting bioapplications of nanoparticles refers to “magnetic fluid hyperthermia” (MFH), i.e. the controlled heating of tumour tissue. In this therapy, magnetic nanoparticles penetrate into the tumour tissue and are inductively heated by applying AC magnetic fields. The biggest challenge of MFH therapy is the temperature control for which fiberoptical thermometers must be inserted into the tumour. A potential way to overcome this problem seems to be the application of carbon nanotubes filled with iron, which could provide in-situ temperature control, with use of an external magnetic field, which allow its manipulation in deep layers of human tissue. The temperature can be detected e.g. by NMR where different characteristics of the material can be investigated (NMR shift, relaxation times, quadrupolar splitting or linewidth). Iron used as filler is a promising candidate due to its ferromagnetic behaviour. In order to apply this kind of system as a magnetic nano-heater and a drug delivery carrier in medical diagnosis and therapeutic treatment at the cellular level, the pure and bulk scale synthesis of such a molecular system is crucial.

Various efforts have been made for the synthesis of iron filled MWCNT and several methods were employed in their production, the most popular being arc-discharge, laser-ablation and chemical vapour deposition (CVD) [1]. The CVD method in comparison with other techniques attracts the biggest attention due to its upward scalability, low cost, use of low temperatures and bulk scale production of carbon nanotubes [2–8].

\* Corresponding author: e-mail: eborowiak@ps.pl

Despite many experimental studies on Fe-MWCNT synthesis, the preparation of a sample with the high purity and yield on a bulk scale still remains a challenge. Here, we present a synthesis route and an efficient purification procedure for Fe-MWCNT. The importance of the study comes from the systematic analysis of the influence of the acid treatment for the stability of the filler and the purity of the material on a bulk scale. In addition, the bulk and local scale analysis of iron phase resulted in the formation of ferromagnetic  $\alpha$ -phase iron nanowires incorporated into the tubes.

## 2 Experimental

The sample was synthesized via the catalytic decomposition of ferrocene under a methane gas flow in a quartz tube reactor inside a dual zone furnace. Ferrocene is the iron source while methane acts as the carbon feedstock and the carrier gas. The main parameters are the sublimation temperature of ferrocene (applied in the first furnace stage), the deposition temperature (in the second furnace stage),  $T = 174\text{ }^{\circ}\text{C}$ ,  $T = 950\text{ }^{\circ}\text{C}$ , respectively. The methane flow rate was 200 ml/min. The reaction time was 0.5 h. Before the process took place, the system was evacuated to ca.  $10^{-3}$  mbar at room temperature.

Annealing in air at  $350\text{ }^{\circ}\text{C}$  for 1 h purified the as-produced material and then various acid treatments (2M, 3M, 4M HCl) were performed for further purification. Afterwards, the product was filtrated, washed thoroughly with distilled water and acetone. The sample was prepared on the standard copper TEM grid and characterized using transmission electron microscopy (TEM), electron energy-loss spectroscopy (EELS) and its high angle annular dark field (HAADF) mode, energy dispersive X-ray (EDX) analysis and selected area electron diffraction (SAED).

## 3 Results and discussion

SEM micrographs of the as-produced Fe-MWCNT showed the presence of impurities in form of the amorphous structures (images not presented here). Therefore, an efficient purification treatment is required. The first step was carried out by annealing in an open furnace at  $350\text{ }^{\circ}\text{C}$  for 1h in order to reduce the amorphous carbon content. The next purification step was an HCl treatment. This stage is crucial in order to remove any excess metallic compounds, which remain on the surface of MWCNT. The importance of this step comes from the fact excessively concentrated acid would also etch away the metal in the interior of the tubes [9]. Hence the right concentration of the applied acid must be found experimentally. From TEM analysis one can observe that the samples treated with 3M and 4M HCl loose the iron not only from the surface of the tubes but also from their interiors (Fig. 1a). On other hand 2M HCl treated sample removes excess iron on the tube surface whilst the filling resists the treatment. Additionally, it is worth noting that the majority of iron particles which are not encapsulated into graphitic onions are removed. Some metal particles, which are encapsulated by graphitic layers still remain in the samples.

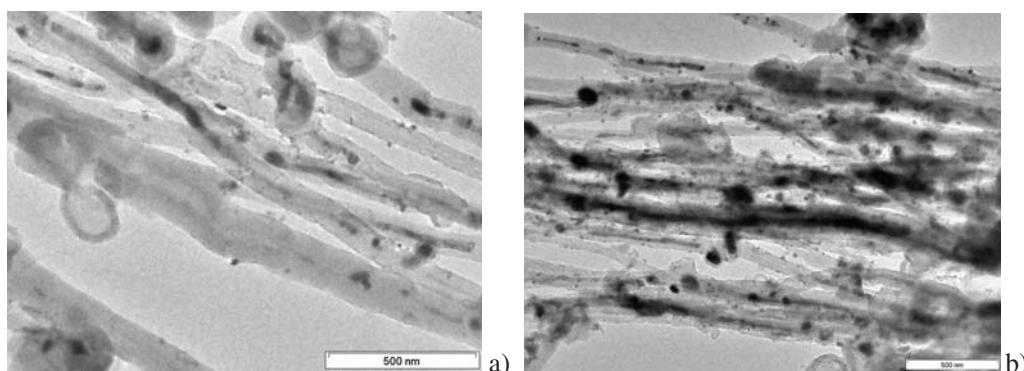


**Fig. 1** Bright field TEM micrographs after purification by HCl (a) 4M and (b) 2M.

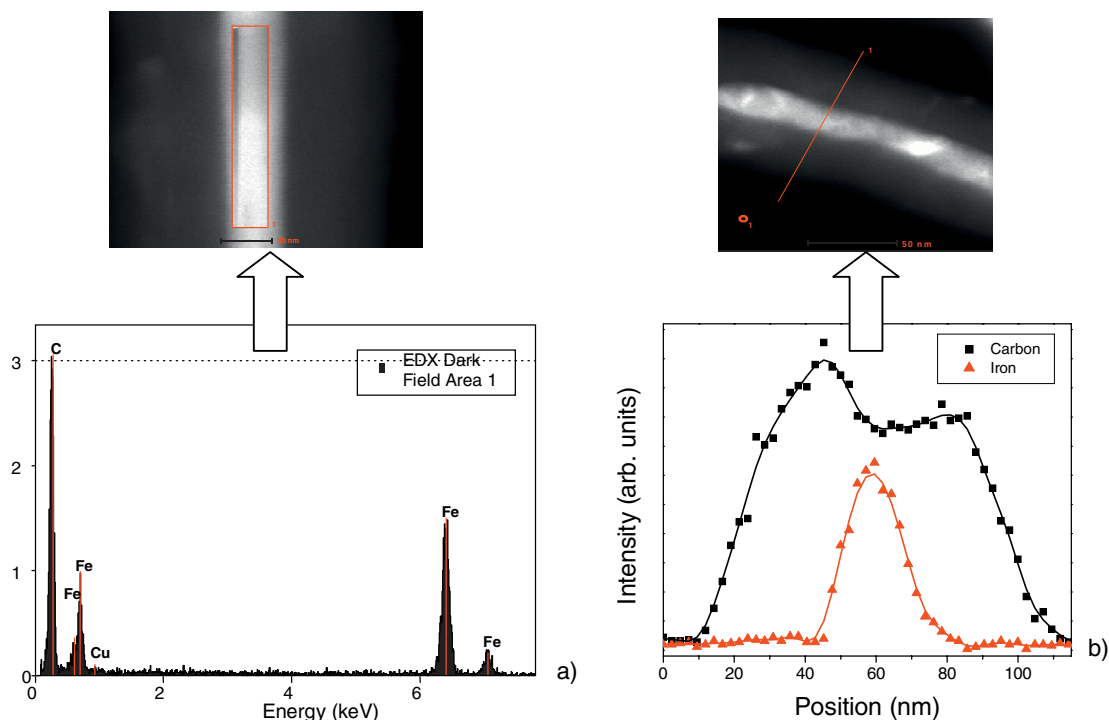


**Fig. 2** (online colour at: [www.pss-b.com](http://www.pss-b.com)) (a) EDX spectrum of  $\alpha$ -Fe-filled nanotubes taken across the bundle from a STEM image (upper panel); (b) distribution of particles along the cross section of a Fe-filled nanotube from a STEM micrograph.

TEM pictures of the samples after 1 h treatment in 2M HCl (Fig. 1b) confirm the above-mentioned observations. All the described experiments were performed for 1 h. Additional experiments with extended process times (20 h and 60 h) for 2M HCl treated sample were also investigated, but no further improvement in the purification was observed.

The chemical composition of the individual tubes filled with metal was performed with EDX analysis (Fig. 2a). The area of the analyzed sample is indicated by the square in the STEM micrograph.

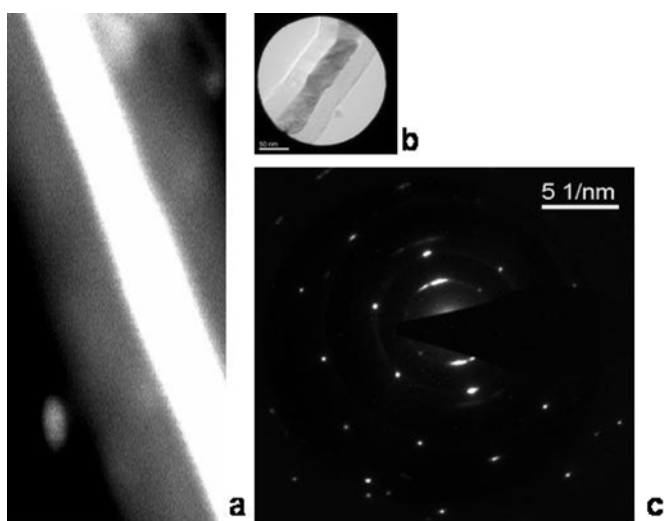


**Fig. 3** HAADF image (a) and SAED pattern (c) from the selected area shown in STEM micrograph (b) of iron filled in a single CNT.

analysis reveals that the only detected signals come from iron, carbon and copper (from TEM grid). Further confirmations of the chemical composition and profile concentration were performed using local EELS (Fig. 2b) [10]. Here the investigation of the correlation of the carbon and iron signal with EELS is demonstrated. The Fe and C profiles show a clear correlation between them, while their maximum intensities are anti-correlated.

The iron phase identification of the individual object was conducted with the selected area electron diffraction (SAED) technique. The SAED pattern (Fig. 3c) indicates that iron inside the CNT exists in a single crystal, similar to what was reported before [11–15]. The SAED pattern corresponds to the (111) plane of  $\alpha$ -Fe. The  $\alpha$ -Fe phase (body centred cubic (bcc) structure) is thermodynamically and ferromagnetically the most stable form of iron at room temperature. The nanotube walls are almost parallel to the (110) plane of  $\alpha$ -Fe and their growth is shown to be parallel to the (121) plane, direction of the iron. Other common structures found in Fe-MWCNT are  $\gamma$ -Fe [14], or  $\alpha$ -Fe plane (010) [16] and these were not observed in samples. The presence of  $\alpha$ -Fe is confirmed by X-ray Diffraction analysis (data not shown here).

## 4 Conclusions

We have successfully synthesized single phase  $\alpha$ -Fe-filled MWCNT on a bulk scale. The systematic study of the acid treatment in the purification procedure allows us to find the optimum hydrochloric acid concentration. The application of 2M HCl solution resulted in a significant reduction of the external iron products, while the iron inside the tubes was not etched away. Increasing the length of time for this acid treatment did not improve purity of the sample. We believe that presented study is a step forward to the application of these materials as nano-heaters in the biomedical field of anti-cancer therapy.

**Acknowledgement** Research was supported by the European Community through the Marie Curie Research Training Network CARBIO under Contract MRTN-CF-2006-035616.

## References

- [1] A. Barreiro, D. Selbmann, T. Pichler, K. Biedermann, T. Gemming, M. Rummeli, U. Schwalke, and B. Buchner, *Appl. Phys. A* **82**, 719–725 (2006).
- [2] A. Leonhardt, M. Ritschel, R. Kozhuharova, A. Graff, T. Muhl, R. Huhle, I. Monch, D. Elefant, and C. Schneider, *Diam. Relat. Mater.* **12**, 790–793 (2003).
- [3] A. Barreiro, S. Hampel, M. H. Rummeli, C. Kramberger, A. Gruneis, K. Biedermann, A. Leonhardt, T. Gemming, B. Buchner, A. Bachtold, and T. Pichler, *J. Phys. Chem. B* **110**, 20973–20977 (2006).
- [4] H. Kim and W. Sigmund, *Carbon* **43**, 1743–1748 (2005).
- [5] F. Geng and H. Cong, *Physica B* **382**, 300–304 (2006).
- [6] S. Hampel, A. Leonhardt, D. Selbmann, K. Biedermann, D. Elefant, C. Muller, T. Gemming, and B. Buchner, *Carbon* **44**, 2316–2322 (2006).
- [7] Yu-Lin Hsin, Jyun-Yi Lai, Kuo Chu Hwang, Shen-Chuan Lo, Fu-Rong Chen, and J. J. Kai, *Carbon* **44**, 3328–3335 (2006).
- [8] H. Hou, A. K. Schaper, F. Weller, and A. Greiner, *Chem. Mater.* **14**, 3990–3994 (2002).
- [9] R. Sen, A. Govindaraj, and C. Rao, *Chem. Phys. Lett.* **267**, 276–280 (1997).
- [10] Ki-Eun Kim, Kang-Jin Kim, Woo Sung Jung, Seung Yong Bae, Jeunghee Park, Junghyun Choi, and Jaebum Choo, *Chem. Phys. Lett.* **401**, 459–464 (2005).
- [11] Keying Shi, Yajuan Chi, Haitao Yu, Baifu Xin, and Honggang Fu, *J. Phys. Chem. B* **109**, 2546–2551 (2005).
- [12] X. P. Gao, Y. Zhang, X. Chen, G. L. Pan, J. Yan, F. Wu, H. T. Yuan, and D. Y. Song, *Carbon* **42**, 47–52 (2004).
- [13] C. H. Liang, G. W. Meng, L. D. Zhang, N. F. Shen, and X. Y. Zhang, *J. Cryst. Growth* **218**, 136–139 (2000).
- [14] Jipeng Cheng, Xiaobin Zhang, Fu Liu, Jiangping Tu, Ying Ye, Yujie Ji, and Changpin Chen, *Carbon* **41**, 1965–1970 (2003).
- [15] C. N. R. Rao, F. L. Deepak, Gautam Gundiah, and A. Govindaraj, *Prog. Solid State Chem.* **31**, 5–147 (2003).
- [16] B. C. Satishkumar, A. Govindaraj, P. V. Vanitha, Arup K. Raychaudhuri, and C. N. R. Rao, *Chem. Phys. Lett.* **362**, 301–306 (2002).